Solar Cells

DOI: 10.1002/anie.201108076

Rapid Charge Transport in Dye-Sensitized Solar Cells Made from Vertically Aligned Single-Crystal Rutile TiO_2 Nanowires**

*Xinjian Feng, Kai Zhu, Arthur J. Frank, Craig A. Grimes, and Thomas E. Mallouk**

Over the past two decades, dye- and quantum dot-sensitized solar cells and polymer/inorganic hybrid solar cells have emerged as promising alternatives to solid-state p-n junction cells for addressing the urgent need for inexpensive, efficient solar power.[1] At the heart of these solar cells is a mesoporous TiO_2 nanoparticle (NP) electrode, which not only provides a high surface area for accommodating the light-absorbing sensitizer but also serves as the stable conductor for photogenerated electrons. Fast charge transport in the network is essential for effective charge collection, particularly in solid-state cells in which recombination is very fast.[2] To increase the electron mobility, TiO_2 1D polycrystalline nanotube arrays[3] and single-crystalline nanowire (NW) arrays[4,5] have recently been proposed and studied as electrode materials for solar cells. However, there is little experimental evidence of substantially enhanced electron transport in these TiO_2 1D nanostructure-based solar cells. For example, there is no substantial difference in electron transport between 1D TiO_2 nanotube and NP-based dye-sensitized solar cells (DSSCs).[3c]

Herein, we report a ketone–HCl solvothermal process for the growth of single-crystal rutile TiO_2 NW arrays on F-doped tin oxide (FTO) substrates. The TiO_2 NWs begin to grow within 15 min and lengths up to 10 μm can be obtained within 2 h. Using these NW films, we show for the first time that the electron diffusion coefficient of single-crystal rutile TiO_2 NWs is more than two orders of magnitude higher than that of rutile NP films at the same photoelectron density. In light of the findings reported here, arrays of 1D single-crystal rutile TiO_2 are attractive for solar cell and other optoelectronic applications.

Figure 1 a,b show, respectively, cross-sectional field-emission scanning electron microscope (FE-SEM; JEOL 6300) images taken at low and high magnification, which show

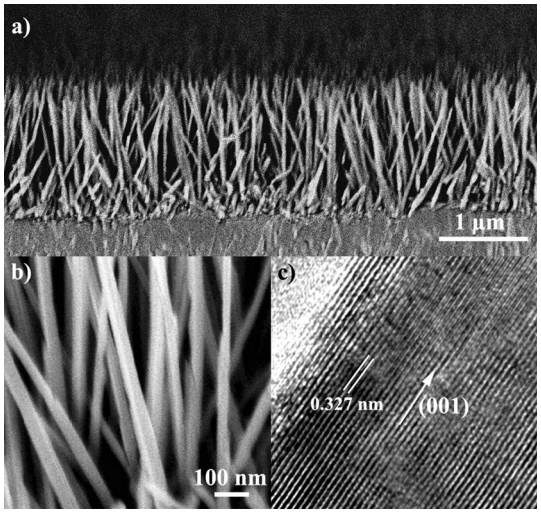

Figure 1. a and b) FE-SEM cross-sectional images of NW arrays on FTO-coated glass substrate at low and high magnifications, respectively. c) HR-TEM image of the as-synthesized single NW.

arrays of uniform and well-separated NWs. NWs grow vertically from the substrate to an average length of about 1.6 μm and a diameter of 40 nm during a reaction time of 30 min. From the grazing angle X-ray diffraction (GAXRD) patterns (Figure S1 in the Supporting Information), the crystal phase of the thin base layer and nanowire arrays were identified as tetragonal rutile (JCPDS file number 21-1276). High-resolution transmission electron microscope (HR-TEM) images (Figure 1 c) confirm that the NWs are single crystalline and have a (110) interplanar distance of 0.327 nm. The NWs grow with a preferred [001] orientation. The length of NWs increases almost linearly with the reaction time. For example, growth of 15 min results in around 260 nm long NWs and a two hour reaction gives around 9.6 μm long NWs (see Figure S2 in the Supporting Information). The NW length can also be adjusted by using different amounts of precursor. For example, for a reaction temperature of 200 °C and a duration of 45 min NWs with lengths of around 1.1 and around 4.4 μm can be obtained by using 0.4 and 0.8 mL of tetrabutyl titanate, respectively (see Figure S3 in the Supporting Information).

[*] Dr. X. Feng,[+] Prof. C. A. Grimes, Prof. T. E. Mallouk
Department of Chemistry, Materials Research Institute
The Pennsylvania State University
University Park, PA 16802 (USA)
E-mail: tem5@psu.edu
Dr. K. Zhu,[+] Dr. A. J. Frank
National Renewable Energy Laboratory
1617 Cole Boulevard, Golden, CO 80401 (USA)
[+] These authors contributed equally to this work.

[**] Work at Penn State was supported by the U.S. Department of Energy, Office of Science, Office of Basic Energy Sciences under grant number DE-SC0001087. Work at NREL was supported by the U.S. Department of Energy, under grant number DEAC36-08GO28308. The Penn State Nanofabrication facility is supported by the National Science Foundation under grant number ECS-0335765. We would like to thank Dr. Bangzhi Liu at the Penn State Nanofabrication facility for his help with FE-SEM, TEM, and HR-TEM analyses.

Supporting information for this article is available on the WWW under http://dx.doi.org/10.1002/anie.201108076.

For most transition-metal oxides, the challenge of controlling crystal orientation and texture arises from the fast hydrolysis and condensation of metal–organic precursors. To control the morphology, strongly acidic media are frequently required, which in turn lead to slow reaction rates. Consequently, reaction times longer than 20 h are usually required.[4] We observe fast growth of NWs using *n*-butanone as solvent. Ketones have previously been used in the nonaqueous sol–gel synthesis of NPs, acting both as the solvent and as a source of oxygen atoms.[6] During the growth of TiO_2 nanocrystals, Cl^- ions selectively adsorb onto the (110) crystal plane, suppressing further growth of that plane, and resulting in the oriented growth of NWs along the [001] direction.[7]

Figure 2a compares the photoelectron density (n) dependence of the electron diffusion coefficient (D) for DSSCs based on rutile NW and NP films. The values of D and n were determined using procedures described in detail elsewhere.[8a,b] The nonlinear dependence of D on the photoelectron density is commonly observed and often ascribed to electrons undergoing multiple trapping–detrapping events within an exponential distribution of conduction band tail states.[8c] The diffusion coefficient in the single-crystal rutile NW-based DSSC is over 200 times higher than that of the rutile NP-based cell[9] at the same photoelectron density (e.g., at $1\times10^{17}\ cm^{-3}$). Over the past two decades, little attention has been paid to rutile TiO_2 nanocrystalline films in DSSCs. The main reason that rutile TiO_2 has been considered uninteresting for DSSCs is its much lower electron diffusion coefficient than the anatase polymorph in both single-crystalline and polycrystalline forms.[10] For rutile nanoparticles in DSSCs, the transport rate is, in part, limited by the low number of interparticle connections.[10c] The dramatically increased electron transport rate for vertical rutile NWs relative to rutile NPs is presumably associated with the lack of grain boundaries along the oriented NWs. The lower density surface defects of the oriented NWs plays a role.

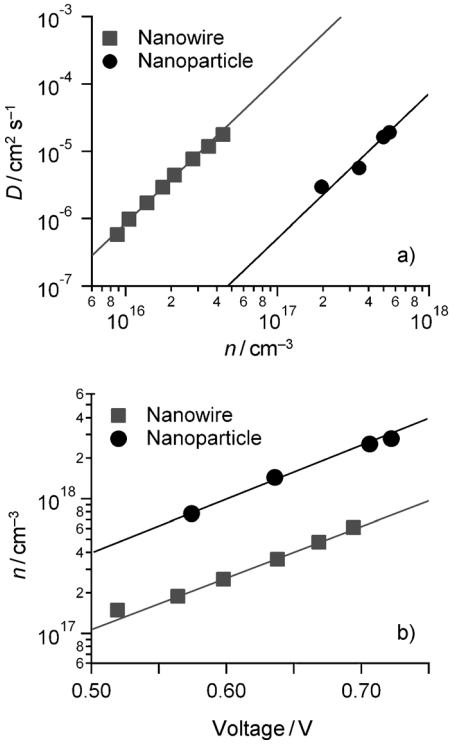

Figure 2. Comparison of a) electron diffusion coefficients (D) as a function of the photoelectron density (n) and b) the photoelectron density as a function of the voltage for rutile NW- and NP-based DSSCs with a laser illumination at 680 nm.

Figure 2b shows the dependence of the photoelectron density n on the voltage for rutile NW- and NP-based DSSCs. The voltage dependence of n (or chemical capacitance) is usually used as a measure of the distribution of sub-bandgap defect states of the electrode materials.[11] The same (parallel) dependence of n on the voltage for these two samples suggests that the shape of the distribution of sub-bandgap states does not depend on the electrode morphology. The photoelectron density in the single-crystal rutile NW-based DSSC is about four times smaller than that in the rutile NP-based cell at the same voltage, indicating that the total density of sub-bandgap defect states in the NW sample is also about four times less than that in the NP sample, which partially accounts for the observed transport properties discussed above.

Figure 3 compares the recombination times (τ_r) for DSSCs based on rutile NWs and NPs as a function of the photoelectron density. At a given photoelectron density (e.g., $1\times10^{18}\ cm^{-3}$) the lifetime in rutile NW-based cells is one order of magnitude shorter than that of rutile NP-based cells. The former can be understood in terms of the electron transport properties shown in Figure 2a. The higher the diffusion coefficient, the faster the photogenerated electrons can reach the anode contact, but faster diffusion also increases the recombination rate of electrons with species at the surface of the particles (e.g., oxidized dye or iodine species), leading to a shorter electron lifetime. The charge collection property of DSSCs can be measured by the electron diffusion length (L_n), which is determined by $L_n=(D\tau_r)^{1/2}$. A longer L_n usually leads to a higher charge-collection efficiency

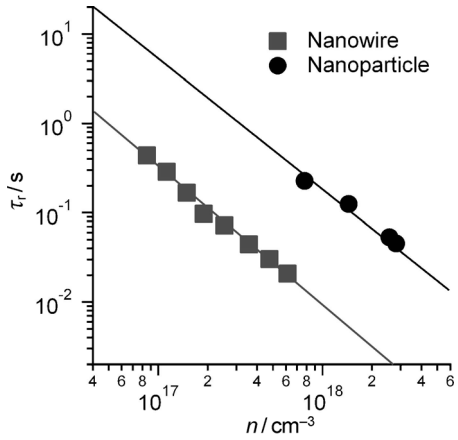

Figure 3. Comparison of recombination lifetimes for rutile NW- and NP-based DSSCs as a function of the photoelectron density with laser illumination at 680 nm.

(η_{cc}). To ensure the optimum cell performance is obtained, L_n is usually several times (e.g., more than three times) greater than the film thickness.[11] Analyses of the data in Figures 2a and 3 yield approximately $L_n = 60\,\mu m$ for the NW-based DSSC and only 13 μm for the NP-based DSSC. Thus, the optimum film thickness would be about 20 and 4 μm for the NW- and NP-based cells, respectively. Thus, the device performance of NW-based cells can be increased by simply increasing the NW film thickness (up to 20 μm) without negatively affecting η_{cc}. In contrast, extending the NP film thickness much beyond 4 μm would significantly reduce η_{cc} and thus lower the device performance.

Figure 4 compares the *J–V* characteristics of NW- and NP-based DSSCs. The film thickness was 4.5 μm for both cells. The DSSC based on a single-crystal rutile NW array showed

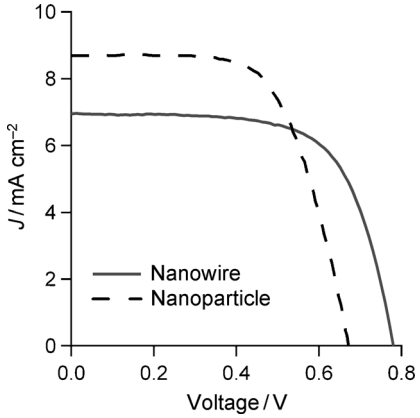

Figure 4. *J–V* characteristics of DSSCs based on a 4.5 μm long NW array and a NP film under simulated AM 1.5 light (J = photocurrent density).

an open-circuit voltage (V_{oc}) of 0.78 V, a fill factor (FF) of 0.68, and a short-circuit photocurrent density (J_{sc}) of 6.95 mA cm^{-2} to give a solar conversion efficiency of 3.68%. In contrast, the DSSC based on a rutile NP film showed a V_{oc} of 0.67 V, a FF of 0.64, and a J_{sc} of 8.70 mA cm^{-2} to yield an efficiency of 3.74%.[9] The 20% less J_{sc} value for the NW-based cell is primarily resulting from its much less surface area than the NP-based cell. However, as the electron diffusion length for cells using NW arrays (60 μm) is more than a factor of four longer than that for cells using NP films (13 μm) and is much longer than the film thickness (4.5 μm) used in this study, we expect that J_{sc} for NW-based cells can be substantially enhanced by increasing the length of NW arrays without lowering their charge-collection efficiencies. The larger FF value for the NW-based DSSC (relative to the NP-based DSSC) is presumably associated with the much increased (by more than two orders of magnitude) transport rate. The NW-based DSSC showed a 110 mV higher V_{oc} than the NP-based DSSC, in agreement with the observed difference in the density of sub-bandgap states between NW- and NP-based cells (Figure 2b). Thus, in comparison to polycrystalline rutile NPs, the single-crystal rutile NW architecture could give higher solar conversion efficiency and is attractive for DSSC applications.

In conclusion, we have developed a ketone-based solvothermal synthesis for single-crystal rutile NWs as vertically oriented arrays on FTO substrates, and for the first time we find that the electronic transport properties of the rutile phase are dramatically improved in DSSCs. In addition, we find that the density of sub-bandgap defect states in the NW-based DSSC is significantly lower than that in the NP-based DSSC. In light of these results along with a good stability and high refractive index of rutile TiO_2, constructing aligned arrays of 1D single-crystal rutile TiO_2 is an attractive approach for solar cell and other optoelectronic applications. The data reported here also suggest that it may be possible, by using a proper texture and crystal orientation, to significantly improve the electrical transport properties of other oxide materials that currently have limited utility in solar cell and related applications because of their low carrier mobility.

Experimental Section

A FTO-coated glass (TEC-8) was cleaned by sonication in acetone, 2-propanol, and methanol. After cleaning, a 20 nm thick TiO_2 layer was deposited by dip-coating (0.3 M tetrabutyltitanate in ethanol) followed by 30 min at 500 °C in air. The substrates were then loaded into a sealed Teflon-lined stainless steel reactor (23 mL volume), containing a mixture of *n*-butanone (6 mL), 37% hydrochloric acid in water (6 mL), and different amounts of tetrabutyl titanate. The reactor was then heated at 200 °C for 15 min to 2 h. The NW samples were then washed with ethanol, dried in air, dipped in a H_2O_2 (30 wt%)/NH_4OH (25 wt%; *v:v* of 10/1) solution for 10 min, rinsed with water and heated in air at 400 °C for 30 min. For use in DSSCs, NWs array samples were coated with dye by immersion overnight at ambient temperature in a 0.5 mM ethanolic solution of commercial N719 dye. The electrolyte was composed of 0.8 M 1-hexyl-2,3-dimethylimidazolium iodide and 50 mM iodine in methoxypropionitrile. A conductive glass slide sputter-coated with 100 nm of Pt was used as the counter-electrode. The thickness of the electrolyte layer between the NW array and counter-electrode was fixed by the use of a 25 μm thick SX-1170 spacer (Solaronix). The photocurrent density and photovoltage of the DSSCs were measured with active sample areas of 0.24–0.5 cm^2 using AM-1.5 simulated sunlight produced by a 500 W Oriel Solar Simulator. Electron transport and recombination properties of DSSCs were measured by intensity-modulated photocurrent and photovoltage spectroscopies as described previously.[8]

Received: November 16, 2011
Published online: February 2, 2012

Keywords: diffusion coefficients · metal oxides · nanoparticles · nanowires · solar cells

[1] a) B. O'Regan, M. Grätzel, *Nature* **1991**, *353*, 737; b) J. Bouclé, P. Ravirajan, J. Nelson, *J. Mater. Chem.* **2007**, *17*, 3141; c) I. Mora-Seró, J. Bisquert, *J. Phys. Chem. Lett.* **2010**, *1*, 3046; d) D. A. R. Barkhouse, R. Debnath, I. J. Kramer, D. Zhitomirsky, A. G. Pattartyus-Abrahan, L. Levina, L. Etgar, M. Grätzel, E. H. Sargent, *Adv. Mater.* **2011**, *23*, 3134.

[2] a) N. Cai, S. J. Moon, L. Cevey-Ha, T. Moehl, R. Humphry-Baker, P. Wang, S. M. Zakeeruddin, M. Grätzel, *Nano Lett.* **2011**, *11*, 1452; b) S. R. Jang, K. Zhu, M. J. Ko, K. Kim, K. C. Kim, N. G. Park, A. J. Frank, *ACS Nano* **2011**, *5*, 8267.

[3] a) D. Gong, C. A. Grimes, O. K. Varghese, W. C. Hu, R. S. Singh, Z. Chen, E. C. Dickey, *J. Mater. Res.* **2001**, *16*, 3331; b) J. M. Macák, H. Tsuchiya, P. Schmuki, *Angew. Chem.* **2005**, *117*, 2136;

Angew. Chem. Int. Ed. **2005**, *44*, 2100; c) K. Zhu, N. R. Neale, A. Miedaner, A. J. Frank, *Nano Lett.* **2007**, *7*, 69.
[4] a) X. J. Feng, K. Shankar, O. K. Varghese, M. Paulose, T. J. Latempa, C. A. Grimes, *Nano Lett.* **2008**, *8*, 3781; b) B. Liu, E. S. Aydil, *J. Am. Chem. Soc.* **2009**, *131*, 3985; c) Z. J. Zhou, J. Q. Fan, X. Wang, W. H. Zhou, Z. L. Du, S. X. Wu, *ACS Appl. Mater. Interfaces* **2011**, *3*, 4349.
[5] a) T. Kasuga, M. Hiramatsu, A. Hoson, T. Sekino, K. Niihara, *Adv. Mater.* **1999**, *11*, 1307; b) C. C. TsaI, H. Teng, *Chem. Mater.* **2006**, *18*, 367; c) J. E. Boercker, E. Enache-Pommer, E. S. Aydil, *Nanotechnology* **2008**, *19*, 095604.
[6] M. Niederberger, G. Garnweitner, *Chem. Eur. J.* **2006**, *12*, 7282.
[7] M. Adachi, Y. Murata, J. Takao, J. T. Jiu, M. Sakamoto, F. M. Wang, *J. Am. Chem. Soc.* **2004**, *126*, 14943.
[8] a) J. van de Lagemaat, N. G. Park, A. J. Frank, *J. Phys. Chem. B* **2000**, *104*, 2044; b) K. Zhu, N. Kopidaks, N. R. Neale, J. van de Lagemaat, A. J. Frank, *J. Phys. Chem. B* **2006**, *110*, 25174; c) A. J. Frank, N. Kopidakis, J. van de Lagemaat, *Coord. Chem. Rev.* **2004**, *248*, 1165.
[9] N. G. Park, G. Schlichthorl, J. van de Lagemaat, H. M. Cheong, A. Mascarenhas, A. J. Frank, *J. Phys. Chem. B* **1999**, *103*, 3308.
[10] a) H. O. Finklea in *Semiconductor Electrodes*, *Studies in Physical and Theoretical Chemistry*, *Vol. 2*, Elsevier, Amsterdam, **1988**, p. 3; b) L. Forro, O. Chauvet, D. Emin, L. Zuppiroli, H. Berger, F. Lévy, *J. Appl. Phys.* **1994**, *75*, 633; c) N. G. Park, J. van de Lagemaat, A. J. Frank, *J. Phys. Chem. B* **2000**, *104*, 8989; d) S. Kambe, S. Nakade, Y. Wada, T. Kitamura, S. Yanagida, *J. Mater. Chem.* **2002**, *12*, 723.
[11] L. M. Peter, *J. Phys. Chem. C* **2007**, *111*, 6601.

